

Well-posed continuum equations for granular flow with compressibility and $\mu(I)$ -rheology

T. Barker¹, D.G. Schaeffer², M. Shearer³ & J.M.N.T Gray¹

¹School of Mathematics and Manchester Centre for Nonlinear Dynamics, University of Manchester, Manchester, UK

²Mathematics Department, Duke University, Durham, NC, USA

³Department of Mathematics, North Carolina State University, Raleigh, NC, USA

Abstract

Continuum modelling of granular flow has been plagued with the issue of ill-posed equations for a long time. Equations for incompressible, two-dimensional flow based on the Coulomb friction law are ill-posed regardless of the deformation, whereas the rate-dependent $\mu(I)$ -rheology is ill-posed when the non-dimensional strain-rate I is too high or too low. Here, incorporating ideas from Critical-State Soil Mechanics, we derive conditions for well-posedness of PDEs that combine compressibility with I -dependent rheology. When the I -dependence comes from a specific friction coefficient $\mu(I)$, our results show that, with compressibility, the equations are well-posed for all deformation rates provided that $\mu(I)$ satisfies certain minimal, physically natural, inequalities.

1 Introduction

Much effort has been devoted to formulating constitutive laws for continuum models of granular materials [1, 2, 3, 4, 5]. However, the lack of acceptable dynamic theories, i.e., well posed equations in the sense of Joseph & Saut [6], for granular flow has severely hampered progress in modelling many geophysical and industrial problems. In the simplest class of models, flow is described by Partial Differential Equations (PDEs) for the density, the velocity vector and the stress tensor; conceptually, such models are hardly more complicated than the Navier–Stokes equations. The equations represent conservation

laws for mass and momentum coupled to constitutive equations to close the system. However, despite the appeal of their simplicity, they have been plagued with ill-posedness, i.e. small perturbations grow at an unbounded rate in the limit that their wavelength tends to zero [6]. Such behaviour is clearly unphysical. However, the immediate practical implication of ill-posedness is that numerical computations either blow-up, even at finite resolution, or do not converge to a well-defined solution as the grid is refined, i.e. the numerical results are grid dependent [7, 8, 9].

The first model of this type [2, 10, 11] specifies constitutive laws that represent a tensorial generalisation of the work of de Coulomb [12] on earthwork fortifications. In the language of plasticity theory, it is a rate-independent, rigid/perfectly-plastic model with a yield condition based on friction between the grains. However, it was shown to be ill-posed in all two-dimensional contexts and all realistic three-dimensional contexts [2]. Critical State Soil Mechanics [1] is a sophisticated elaboration of Coulomb behaviour that allows for compressibility. It also suffers from ill-posedness, depending of the degree of consolidation. This ill-posedness is much less severe than for a Coulomb material [11, 3], but still bad enough to block its use in applications. More recently, the $\mu(I)$ -rheology [4, 13, 5] introduces a modest amount of rate dependence into (incompressible) Coulomb behaviour through the non-dimensional *inertial number*, which is proportional to the shear-rate and inversely proportional to the square-root of the pressure. As shown in Barker *et al.* [9], this theory leads to well posed (two-dimensional) equations in a significant region of state space, but it is ill-posed at both low and high inertial numbers.

This paper is centred on formulating constitutive equations that extend the incompressible $\mu(I)$ -rheology of Jop *et al.* [5] to compressible deformations, by combining it with Critical State Soil Mechanics. The main result is that in two dimensions, the new model is well-posed for all densities, for all stress states, and for all deformation rates. In other words, to obtain well-posedness, we modify Coulomb behaviour by including only two natural, fairly small, perturbations of the theory, namely compressibility and rate dependence. This has the advantage that it retains the conceptual simplicity of the original theory. Although we consider only two-dimensional flow, it should be noted that in numerous cases it has been found that flow in two dimensions is more prone to ill-posedness than in three [2, 3, 14]. Thus, we anticipate that the corresponding three-dimensional equations including these effects will also be well posed.

Currently a wide range of new constitutive laws for granular materials are being developed including the $\mu(I)$ -rheology [4, 5], elasto-plastic formulations [15, 16] non-local rheologies [17, 18, 19, 20], kinetic theory [21], as well as Cosserat [22], micro-structural [23] and hypoplastic theories [24]. Enormous progress has been made over the past decade and there is the realistic and exciting prospect that practical granular flows, that span the solid-like, liquid-like and gaseous regimes, may shortly be described by continuum models. In this paper we seek to understand one of the conceptually simplest formulations that leads to well-posed equations.

In Section 2 we introduce the equations to be studied and formulate our well-posedness result for

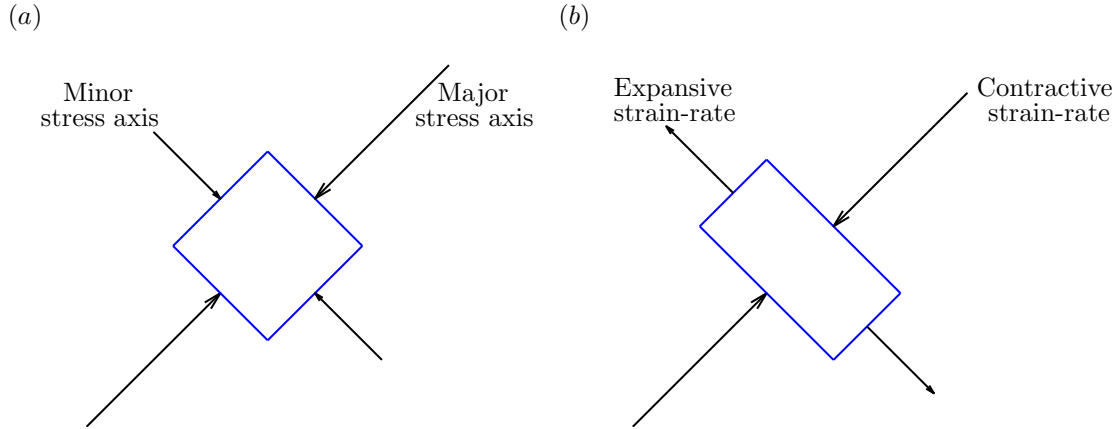


Figure 1: (a) Illustrative stress eigenvectors; along the major axis the stress eigenvalue is $-(p + \|\boldsymbol{\tau}\|)$ with the minus sign indicating compression. (b) A possible material deformation that is consistent with the stress field in (a).

them. This theorem is proved in Sections 3 and 4. In two appendices we summarise key ideas from Critical State Soil Mechanics and survey topics regarding ill-posed partial differential equations.

2 Governing equations

Dense granular flow is described by the solids-volume fraction ϕ , the velocity vector \mathbf{u} , and the stress tensor $\boldsymbol{\sigma}$. In two dimensions this constitutes six scalar unknowns that are spatially and temporally dependent. These are governed by conservation laws plus constitutive relations. Conservation of mass gives the scalar equation

$$(\partial_t + u_j \partial_j) \phi + \phi \operatorname{div} \mathbf{u} = 0, \quad (1)$$

and conservation of momentum gives the vector equation

$$\rho_* \phi (\partial_t + u_j \partial_j) u_i = \partial_j \sigma_{ij} + \rho_* \phi g_i, \quad (2)$$

where ρ_* is the constant intrinsic density and \mathbf{g} is the acceleration due to gravity. Closure of these equations is achieved through three constitutive relations.

2.1 The Coulomb constitutive model

For a Coulomb material, which is assumed to be incompressible, the first constitutive relation states that ϕ is a constant. This then reduces (1) to the

$$\text{Flow rule:} \quad \operatorname{div} \mathbf{u} = 0. \quad (3)$$

For the next constitutive relation the stress tensor

$$\sigma_{ij} = -p\delta_{ij} + \tau_{ij}, \quad (4)$$

is decomposed into a pressure term (where $p = -\sigma_{ii}/2$) plus a trace-free tensor $\boldsymbol{\tau}$, called the deviatoric stress. The second relation is then the

$$\textbf{Yield condition:} \quad \|\boldsymbol{\tau}\| = \mu p, \quad (5)$$

where μ is a constant and for any tensor \boldsymbol{T} the norm is defined by

$$\|\boldsymbol{T}\| = \sqrt{T_{ij}T_{ij}/2}. \quad (6)$$

This yield condition expresses the idea that a granular material cannot deform unless the shear stress is sufficient to overcome friction¹. The third constitutive relation requires that the eigenvectors of the deviatoric stress tensor and the deviatoric strain-rate tensor²

$$D_{ij} = \frac{1}{2}(\partial_j u_i + \partial_i u_j) - \frac{1}{2}(\text{div } \mathbf{u})\delta_{ij}, \quad (7)$$

are aligned (see Figure 1 for motivation), which may be written

$$\textbf{Alignment:} \quad \frac{D_{ij}}{\|\boldsymbol{D}\|} = \frac{\tau_{ij}}{\|\boldsymbol{\tau}\|}. \quad (8)$$

In words (8) may be interpreted as asserting that in the space of trace-free symmetric 2×2 matrices, *which is two-dimensional*, \boldsymbol{D} and $\boldsymbol{\tau}$ are parallel. Thus, this matrix equation entails only one scalar relation. For reference below we record that

$$\boldsymbol{D} = \frac{1}{2} \begin{bmatrix} \partial_1 u_1 - \partial_2 u_2 & \partial_1 u_2 + \partial_2 u_1 \\ \partial_1 u_2 + \partial_2 u_1 & \partial_2 u_2 - \partial_1 u_1 \end{bmatrix}. \quad (9)$$

It is customary [2], [5] to process these equations by expressing the deviatoric stress $\boldsymbol{\tau}$ in terms of p and the strain rate as follows:

$$\tau_{ij} = \|\boldsymbol{\tau}\| \frac{\tau_{ij}}{\|\boldsymbol{\tau}\|} = \mu p \frac{D_{ij}}{\|\boldsymbol{D}\|}, \quad (10)$$

where we have invoked (5) and (8). We may substitute (10) into (2) to obtain

$$\rho_* \phi (\partial_t + u_j \partial_j) u_i = \partial_j \left[\frac{\mu p}{\|\boldsymbol{D}\|} D_{ij} \right] - \partial_i p + \rho_* \phi g_i, \quad (11)$$

and the resulting equation, together with (3), gives three equations for pressure p and velocity \mathbf{u} . In form, at least, these equations resemble the incompressible Navier-Stokes equation. However, in two dimensions (as considered here) they are always ill-posed [2].

¹Thus, (5) contains the implicit assumption that material is actually deforming. Otherwise (5) must be replaced by inequality, $\|\boldsymbol{\tau}\| \leq \mu p$, and the governing equations are underdetermined unless further relations, such as those of elasticity, are included.

²Note that for incompressible flow, the full strain-rate tensor $(\partial_j u_i + \partial_i u_j)/2$ and the deviatoric strain-rate tensor are equal since the second term on the right in (7) vanishes.

2.2 Incompressible $\mu(I)$ -rheology

Work described by the Groupement De Recherche Milieux Divisés [4] has significantly improved the Coulomb model by including some rate dependence (in the sense of plasticity [25]) in the yield condition while making no changes in the incompressible flow rule (3) and the alignment condition (8). Specifically, a wide range of experiments is captured by replacing the constant μ in (5) by an increasing function $\mu(I)$ of the *inertial number*,

$$I = \frac{2d\|\mathbf{D}\|}{\sqrt{p/\rho_*}}, \quad (12)$$

where d is the particle diameter. The expression

$$\mu(I) = \mu_1 + \frac{\mu_2 - \mu_1}{I_0/I + 1}, \quad (13)$$

where μ_1 , μ_2 and I_0 are constants with $\mu_2 > \mu_1$, is a frequently used form [26]. Below we shall assume that

$$\mu'(I) > 0 \quad \text{and} \quad \mu''(I) < 0. \quad (14)$$

The modified yield condition changes (11) to read

$$\rho_*\phi(\partial_t + u_j\partial_j)u_i = \partial_j \left[\frac{\mu(I)p}{\|\mathbf{D}\|} D_{ij} \right] - \partial_i p + \rho_*\phi g_i. \quad (15)$$

The effect of this seemingly small perturbation is profound. Unlike for Coulomb material, equations (15) and (3) are well-posed for a significant range of inertial numbers, specifically when the deformation rate is neither too small nor too large relative to the pressure [9].

2.3 Compressibility and I -dependent rheology

We refer to Critical State Soil Mechanics (cf. Appendix 1) for guidance in introducing compressibility into the rheology. Thus, we make no change in the alignment condition (8); we assume ϕ -dependence in the yield condition,

$$\|\boldsymbol{\tau}\| = Y(p, \phi, I); \quad (16)$$

and we allow for volumetric changes by introducing a new function $f(p, \phi, I)$ and modifying the flow rule to

$$\text{div } \mathbf{u} = 2f(p, \phi, I) \|\mathbf{D}\|. \quad (17)$$

To get well posed equations, we require that the yield condition and the flow-rule functions are related by the equation³

$$\frac{\partial Y}{\partial p} - \frac{I}{2p} \frac{\partial Y}{\partial I} = f + I \frac{\partial f}{\partial I}, \quad (18)$$

and that they satisfy the inequalities

$$(a) \partial_I Y > 0 \quad \text{and} \quad (b) \partial_p f - \frac{I}{2p} \partial_I f < 0. \quad (19)$$

³If Y and f are independent of I , then (18) leads to the CSSM flow rule (71) derived from normality.

We may now state our main result, the well posedness theorem for the system (1), (2), (8), (16), (17), which we call the CIDR equations. (Mnemonic: compressible I -dependent rheology.) The term *linearly well posed* is defined in Appendix 2, and the result is proved in Sections 3 and 4.

Theorem *Under hypotheses (18) and (19), the CIDR system is linearly well posed.*

Remark: The I -dependence in these equations need not relate to a friction coefficient $\mu(I)$. In §2.5 we connect the equations to $\mu(I)$ -rheology.

2.4 Derivation of evolution equations

To place the equations in a larger continuum-mechanics context, we show that the CIDR equations of motion can be rewritten as a system of three evolution equations for the velocity \mathbf{u} and the solids fraction ϕ . In form, these equations are analogous to the Navier-Stokes equations for a viscous, compressible fluid. We make no use of this form of the equations in our proof of well-posedness.

We want to eliminate stresses from the equations of motion. To this end, we propose to solve for the mean stress p using the flow rule (17), which we rewrite as

$$f(p, \phi, I) = \frac{\operatorname{div} \mathbf{u}}{2\|\mathbf{D}\|}. \quad (20)$$

Note that $f(p, \phi, I)$ depends on p both directly in its first argument and indirectly through $I = 2d\|\mathbf{D}\|/\sqrt{p/\rho_*}$ in its third argument. However,

$$\frac{\partial}{\partial p}[f(p, \phi, 2d\|\mathbf{D}\|/\sqrt{p/\rho_*})] = \partial_p f - \frac{I}{2p} \partial_I f, \quad (21)$$

which by assumption (19b) is nonzero. Thus, we may apply the Implicit Function Theorem to (20) to solve $p = P(\nabla \mathbf{u}, \phi)$.⁴ Given this, we may define

$$T(\nabla \mathbf{u}, \phi) = Y(P(\nabla \mathbf{u}, \phi), \phi, I(\nabla \mathbf{u}, \phi)) \quad \text{where} \quad I(\nabla \mathbf{u}, \phi) = \frac{2d\|\mathbf{D}\|}{\sqrt{P(\nabla \mathbf{u}, \phi)/\rho_*}},$$

and substitute into conservation of momentum to obtain an equation

$$\rho_* \phi (\partial_t + u_j \partial_j) u_i = \partial_j \left[\frac{T(\nabla \mathbf{u}, \phi)}{\|\mathbf{D}\|} D_{ij} \right] - \partial_i [P(\nabla \mathbf{u}, \phi)] + \rho_* \phi g_i. \quad (22)$$

This equation, along with (1), gives a system of three evolution equations for the velocity \mathbf{u} and the solids fraction ϕ .

2.5 Connection to $\mu(I)$ -rheology

Without making any attempt to be general, we illustrate one example of how $\mu(I)$ -rheology may be included in constitutive relations of the form (16), (17). Motivated by equation (72) in Appendix 1, we

⁴Note that P in fact depends only on $\operatorname{div} \mathbf{u}$, $\|\mathbf{D}\|$ and ϕ .

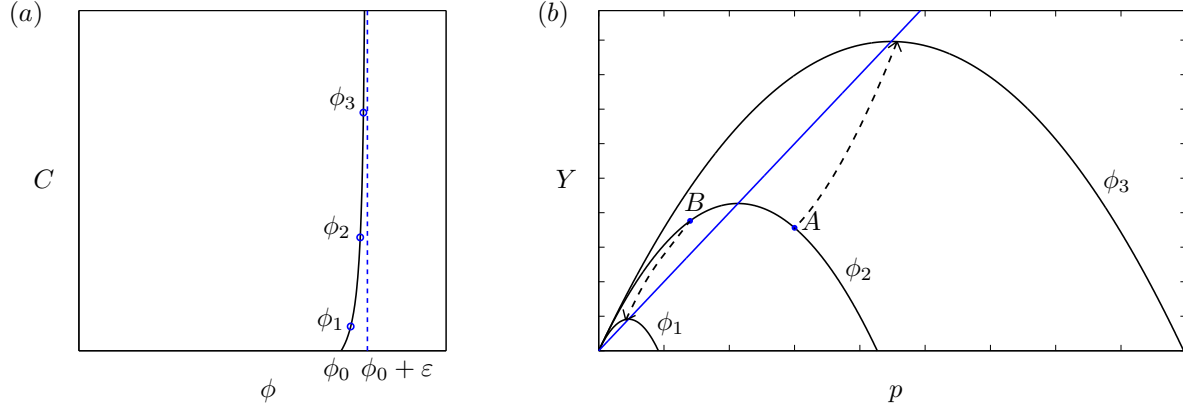


Figure 2: (a) An example curve for the function $C(\phi)$ with a minimum solids volume fraction ϕ_0 and a vertical asymptote at $\phi_0 + O(\varepsilon)$. (b) Nested yield surfaces of the form (23) for a fixed value of I with differing solids volume fractions. (The solid blue line, the dashed arrows, and the labels A and B refer to a discussion of CSSM in the Appendix 1.)

make the ansatz

$$(a) \quad Y(p, \phi, I) = \alpha(I)p - p^2/C(\phi) \quad (23)$$

$$(b) \quad f(p, \phi, I) = \beta(I) - 2p/C(\phi).$$

In these equations, it is worth emphasising that p, ϕ, I are treated as independent variables, not to be confused with the dependence of I on p in the previous subsection. The function $C(\phi)$ is an increasing function of ϕ . As ϕ varies (with I fixed) the yield loci $\|\boldsymbol{\tau}\| = Y(p, \phi, I)$ derived from (23a) form a nested family of convex curves in stress space (cf. Figure 2(b)). Observe from (17) that deformation without volumetric strain is possible if $f(p, \phi, I) = 0$; i.e., for (23b), if $p/C(\phi) = \beta(I)/2$. Substituting this formula into (16) and using (23a), we derive

$$\|\boldsymbol{\tau}\| = [\alpha(I) - \beta(I)/2] p$$

for such isochoric deformation to be possible. Thus, to recover the yield condition $\|\boldsymbol{\tau}\| = \mu(I)p$ of the $\mu(I)$ -rheology, let us require that

$$\alpha(I) - \beta(I)/2 = \mu(I). \quad (24)$$

Lemma 1. Equations (18) and (24) imply that

$$\alpha(I) = \frac{4}{5}\mu(I) + \frac{12}{25}I^{-2/5} \int_0^I \tilde{I}^{-3/5} \mu(\tilde{I}) d\tilde{I} \quad (25)$$

and

$$\beta(I) = -\frac{2}{5}\mu(I) + \frac{24}{25}I^{-2/5} \int_0^I \tilde{I}^{-3/5} \mu(\tilde{I}) d\tilde{I}. \quad (26)$$

Proof: Substituting the relations (23) into (18), and using (24) to eliminate β , we derive the linear ordinary differential equation for $\alpha = \alpha(I)$:

$$\frac{5}{2}I\alpha'(I) + \alpha(I) = 2\mu(I) + 2I\mu'(I). \quad (27)$$

Solving this linear equation for $\alpha(I)$, with an integrating factor, we obtain

$$I^{2/5}\alpha(I) = \frac{4}{5} \int_0^I \tilde{I}^{-3/5}\mu(\tilde{I})d\tilde{I} + \frac{4}{5} \int_0^I \tilde{I}^{2/5}\mu'(\tilde{I})d\tilde{I},$$

from which the formula (25) follows after integrating the second integral by parts. Finally, substituting this formula for $\alpha(I)$ into (24), we obtain the formula (26) for $\beta(I)$. ■

Lemma 2. The yield condition and flow-rule function (23a,b) that follow from (25), (26) verify hypotheses (18) and (19), provided $\mu(I)$ satisfies (14).

Proof: Of course (18) is satisfied because this equation was imposed in deriving (25), (26).

Differentiating (23b), we see that $\partial_p f(p, \phi, I) = -2/C(\phi) < 0$. To calculate $\partial_I f(p, \phi, I)$, we first reparametrize the integral in (26) to obtain $\beta(I) = -\frac{2}{5}\mu(I) + \frac{24}{25} \int_0^1 s^{-3/5}\mu(sI)ds$. Then

$$\partial_I f(p, \phi, I) = \beta'(I) = -\frac{2}{5}\mu'(I) + \frac{24}{25} \int_0^1 s^{2/5}\mu'(sI)ds.$$

By (14), $\mu''(I) < 0$, so $\mu'(sI) > \mu'(I)$ for $0 < s < 1$. Thus,

$$\beta'(I) > \mu'(I) \left\{ -\frac{2}{5} + \frac{24}{25} \int_0^1 s^{2/5}ds \right\} = \mu'(I) \left\{ \frac{24}{35} - \frac{2}{5} \right\} > 0,$$

the last inequality using (14). Consequently,

$$\partial_p f(p, \phi, I) - \frac{I}{2p} \partial_I f(p, \phi, I) < 0, \quad (28)$$

proving inequality (19b).

For inequality (19a), we reparametrize the integral (25) and differentiate to obtain

$$\partial_I Y(p, \phi, I) = \alpha'(I)p = p \left(\frac{4}{5}\mu'(I) + \frac{12}{25} \int_0^1 s^{2/5}\mu'(sI)ds \right) > 0,$$

as desired. ■

Based on an analogy with CSSM, let us suppose that $C(\phi)$ is a sensitive function of ϕ , say of the form

$$C(\phi) = \tilde{C} \left(\frac{\phi - \phi_0}{\varepsilon} \right) \quad (29)$$

where ϕ_0 is the minimum solids fraction for sustained stress transmission between grains (random loose packing), ε is a small parameter, and for definiteness we may take $\tilde{C}(z) = z/(1-z)$ as in figure 2. Note that $C(\phi)$ diverges as $\phi \rightarrow \phi_0 + \varepsilon$; thus, (29) requires that ϕ is confined to a narrow range,

$$\phi_0 \leq \phi < \phi_0 + \varepsilon. \quad (30)$$

In physical terms, the maximum solids fraction $\phi_0 + \varepsilon$ represents the jamming threshold. We call the limit $\varepsilon \rightarrow 0$ *incompressible* because, as may be seen from (30), the density of material becomes essentially constant.

Lemma 3. As $\varepsilon \rightarrow 0$, the CIDR equations reduce to the equations of incompressible $\mu(I)$ -rheology, (3), (15).

Proof: We process the CIDR equations, which have the six unknowns ϕ , u_i , and σ_{ij} , as follows. First we reduce to five unknowns— ϕ , u_i , p and $\tau = \|\boldsymbol{\tau}\|$ —by recalling the definition (4) and the alignment condition (8) to write

$$\sigma_{ij} = -p\delta_{ij} + \tau \frac{D_{ij}}{\|\mathbf{D}\|}.$$

Next we use the yield condition to eliminate ϕ , reducing this number to four. Specifically, substituting (23a) into (16), we write the yield condition

$$\tau = \alpha(I)p - p^2/C(\phi). \quad (31)$$

Solving (31) for ϕ we obtain

$$\phi = \Phi(\nabla \mathbf{u}, p, \tau) = C^{-1} \left(\frac{p^2}{\alpha(I)p - \tau} \right), \quad (32)$$

where the dependence on $\nabla \mathbf{u}$ comes from the fact that $I = 2d\|\mathbf{D}\|/\sqrt{p/\rho_*}$. Substitution of this formula into the conservation laws (1), (2) yields the equations

$$(\partial_t + u_j \partial_j) \Phi(\nabla \mathbf{u}, p, \tau) + \Phi(\nabla \mathbf{u}, p, \tau) \operatorname{div} \mathbf{u} = 0, \quad (33a)$$

$$\rho_* \Phi(\nabla \mathbf{u}, p, \tau) (\partial_t + u_j \partial_j) u_i = \partial_j \left[\frac{\tau}{\|\mathbf{D}\|} D_{ij} \right] - \partial_i p + \rho_* \Phi g_i. \quad (33b)$$

Finally, we show the flow rule (17) may be rewritten

$$\operatorname{div} \mathbf{u} = 4[\tau/p - \mu(I)] \|\mathbf{D}\|. \quad (34)$$

To see this, we combine (23b) with (24) to conclude

$$f(p, \phi, I) = \beta(I) - 2p/C(\phi) = 2[\alpha(I) - \mu(I)] - 2p/C(\phi)$$

and substitute the relation $\alpha(I) = \tau/p + p/C(\phi)$ derived by manipulating (31). Thus, the system (33), (34) governs the evolution of the four unknowns u_i , p , and τ .

Now we claim that if $C(\phi)$ has the form (29), then (33), (34) is a singular perturbation of (3), (15). It follows from (29) that (32) has the expansion

$$\phi = \phi_0 + \varepsilon \tilde{\Phi}(\nabla \mathbf{u}, p, \tau), \quad (35)$$

where $\tilde{\Phi}(\nabla \mathbf{u}, p, \tau) = \tilde{C}^{-1}(p^2/[\alpha(I)p - \tau])$. Substituting (35) into the continuity equation (33a) we find

$$\varepsilon(\partial_t + u_j \partial_j) \tilde{\Phi}(\nabla \mathbf{u}, p, \tau) + [\phi_0 + \varepsilon \tilde{\Phi}(\nabla \mathbf{u}, p, \tau)] \operatorname{div} \mathbf{u} = 0.$$

If $\varepsilon = 0$ then this equation reduces to $\operatorname{div} \mathbf{u} = 0$, although this is of course a highly singular limit. Thus, if $\varepsilon = 0$, the left hand side of (34) vanishes, so this equation simplifies to the yield condition $\tau = \mu(I)p$, and substitution into (33b) yields (15). This proves the lemma. ■

3 Proofs, Part I: Linearization

3.1 An alternative formulation of the alignment condition

It is convenient to study the linearized equations with a reformulated alignment condition that describes stress in terms of eigenvectors of, rather than entries of, the stress tensor. Since $\boldsymbol{\tau}$ defined by (4) has trace zero, it has eigenvalues⁵ $\pm \|\boldsymbol{\tau}\|$. Taking ψ as the angle that the eigenvector with eigenvalue $-\|\boldsymbol{\tau}\|$ makes with the x_1 -axis gives

$$\boldsymbol{\tau} = -\|\boldsymbol{\tau}\| \begin{bmatrix} \cos 2\psi & \sin 2\psi \\ \sin 2\psi & -\cos 2\psi \end{bmatrix}, \quad (36)$$

which may be verified by checking that $(\cos \psi, \sin \psi)$ is an eigenvector of this matrix with eigenvalue $-\|\boldsymbol{\tau}\|$. Thus, the stress tensor σ_{ij} is completely specified by the three scalars p , $\|\boldsymbol{\tau}\|$, and ψ .

Focusing on the first rows of the strain-rate tensor (9) and of (36), we extract from the matrix equation (8) the vector equation

$$(\partial_1 u_1 - \partial_2 u_2, \partial_1 u_2 + \partial_2 u_1) = k(\cos 2\psi, \sin 2\psi), \quad (37)$$

where $k = -2\|\mathbf{D}\| < 0$. Since \mathbf{D} and $\boldsymbol{\tau}$ lie in the two-dimensional space of trace-free, symmetric matrices, (37) is equivalent to (8). It follows from (37) that

$$\text{Alt. alignment:} \quad (\partial_1 u_2 + \partial_2 u_1) \cos 2\psi - (\partial_1 u_1 - \partial_2 u_2) \sin 2\psi = 0. \quad (38)$$

In point of fact, this equation is slightly weaker than the alignment condition since (38) is consistent with the possibility that $k > 0$ in (37); to rule out the latter possibility we impose the supplemental inequality⁶ that

$$(\partial_1 u_1 - \partial_2 u_2) \cos 2\psi \leq 0. \quad (39)$$

⁵Hence $\boldsymbol{\sigma}$ has eigenvalues $-p \pm \|\boldsymbol{\tau}\|$. Note that $-p - \|\boldsymbol{\tau}\|$ is the major stress eigenvalue—although this eigenvalue is the smaller algebraically, it is the larger in absolute value.

⁶It is also true that $(\partial_1 u_2 + \partial_2 u_1) \sin 2\psi \leq 0$, and if $\cos 2\psi$ were to vanish, we would need to use this inequality to guarantee that $k < 0$. However, this issue will not arise in the analysis below.

3.2 The calculation

Substitution of the stress tensor (36) into the momentum balance equations (2) allows for the full set of equations to be written as

$$\rho_* \phi (\partial_t + u_1 \partial_1 + u_2 \partial_2) u_1 + \partial_1 [p + \tau \cos(2\psi)] + \partial_2 [\tau \sin(2\psi)] = \rho_* \phi g_1, \quad (40a)$$

$$\rho_* \phi (\partial_t + u_1 \partial_1 + u_2 \partial_2) u_2 + \partial_1 [\tau \sin(2\psi)] + \partial_2 [p - \tau \cos(2\psi)] = \rho_* \phi g_2, \quad (40b)$$

$$(\partial_t + u_1 \partial_1 + u_2 \partial_2) \phi + \phi (\partial_1 u_1 + \partial_2 u_2) = 0, \quad (40c)$$

$$\partial_1 u_1 + \partial_2 u_2 = 2f \|\mathbf{D}\|, \quad (40d)$$

$$(\partial_2 u_1 + \partial_1 u_2) \cos(2\psi) + (\partial_2 u_2 - \partial_1 u_1) \sin(2\psi) = 0. \quad (40e)$$

This system has five scalar unknowns, $\mathbf{U} = (u_1, u_2, \phi, p, \psi)$. In (40a),(40b), τ is a mnemonically suggestive abbreviation for the yield function $Y(p, \phi, I)$ in (16), and in (40d), a repetition of (17), the function f depends on arguments (p, ϕ, I) that are not written explicitly.

As in Appendix 2, to linearise the equations we substitute a perturbation of a base solution $\mathbf{U}^{(0)}(\mathbf{x}, t)$, say

$$\mathbf{U} = \mathbf{U}^{(0)} + \hat{\mathbf{U}}, \quad (41)$$

into the equations, retain only terms that are linear in the perturbation $\hat{\mathbf{U}}$, and freeze the coefficients at an arbitrary point (\mathbf{x}^*, t^*) . It is convenient to temporarily drop most terms not of maximal order and estimate their effect in a calculation at the end of the argument. For example, this construction applied to (40c) yields the the constant-coefficient, linear equation

$$(\partial_t + u_1^* \partial_1 + u_2^* \partial_2) \hat{\phi} + \phi^* (\partial_1 \hat{u}_1 + \partial_2 \hat{u}_2) = 0 \quad (42)$$

where $u_j^* = u_j^{(0)}(\mathbf{x}^*, t^*)$ and $\phi^* = \phi^{(0)}(\mathbf{x}^*, t^*)$. Lower-order terms $\partial_j \phi^* \hat{u}_j$ and $\partial_j u_j^* \hat{\phi}$ in the full linearisation of (40c) have been dropped in (42).

In expanding the fully nonlinear factor $\|\mathbf{D}\|$ in (40d), we may take advantage of the rotational invariance of the equations to arrange that $\psi^* = 0$; i.e., we may calculate in a rotated coordinate system for which, at (\mathbf{x}^*, t^*) , the x_1 -axis is the maximal stress axis. Then by the alignment condition (38) the base-state deviatoric strain-rate tensor is diagonal at (\mathbf{x}^*, t^*)

$$\mathbf{D}^* = \begin{bmatrix} (\partial_1 u_1^* - \partial_2 u_2^*)/2 & 0 \\ 0 & (\partial_2 u_2^* - \partial_1 u_1^*)/2 \end{bmatrix}, \quad (43)$$

and by (39), in the 1,1-position of this matrix $\partial_1 u_1^* - \partial_2 u_2^* < 0$. This corresponds to non-zero compression along the major stress axis, as illustrated in Figure 3. Now

$$\|(\mathbf{D}^* + \hat{\mathbf{D}})\| = \frac{1}{2} [(\partial_1 u_1^* - \partial_2 u_2^* + \partial_1 \hat{u}_1 - \partial_2 \hat{u}_2)^2 + (\partial_2 \hat{u}_1 + \partial_1 \hat{u}_2)^2]^{1/2} \quad (44a)$$

$$\approx \|\mathbf{D}^*\| - (\partial_1 \hat{u}_1 - \partial_2 \hat{u}_2)/2, \quad (44b)$$

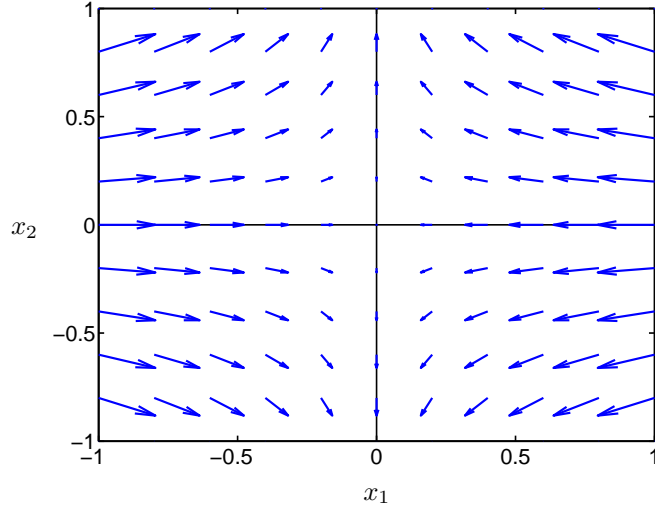


Figure 3: An example of a base-state velocity field for the strain-rate tensor (43) with $\partial_1 u_1^{(0)} \equiv -1$ and $\partial_2 u_2^{(0)} \equiv 1/2$.

where the approximation follows from the expansion

$$\sqrt{(-A + X)^2 + Y^2} = A - X + \mathcal{O}(X^2 + Y^2)$$

if $A > 0$ and $|X|, |Y| \ll A$. Thus, as given in Table 1, the (local) linearisation of $\|\mathbf{D}\|$ equals $-(\partial_1 \hat{u}_1 - \partial_2 \hat{u}_2)/2$.

In (40d) the function f contains p , ϕ , and I as implicit arguments. As reflected in the table, the dependence on p and ϕ contributes zeroth-order terms in these variables to the linearisation.

In (40a), (40b), τ also depends on p , ϕ , and I , and the terms involving τ are differentiated; hence new issues arise in linearising them. For example, by the chain rule,

$$\begin{aligned} \partial_j [\tau \cos(2\psi)] = \cos(2\psi) \left\{ \partial_p \tau \partial_j p + \partial_\phi \tau \partial_j \phi + \partial_I \tau \left[\frac{2d}{\sqrt{p/\rho_*}} \partial_j \|\mathbf{D}\| - \frac{d\|\mathbf{D}\|}{\sqrt{p^3/\rho_*}} \partial_j p \right] \right\} \\ - 2\tau \sin(2\psi) \partial_j \psi. \end{aligned}$$

Since $\psi^* = 0$, the full linearisation of, say, the first term here equals $(\partial_p \tau)^* \partial_j \hat{p}$, a term given in the table, plus lower-order terms

$$(\partial_j p)^* \left\{ (\partial_{pp} \tau)^* \hat{p} + (\partial_{\phi p} \tau)^* \hat{\phi} + (\partial_{Ip} \tau)^* \left[-\frac{I^*}{\|\mathbf{D}^*\|} \hat{D}_{11} - \frac{I^*}{2p^*} \hat{p} \right] \right\}.$$

All of these terms, as well as numerous other analogous terms in the full linearisation of (40a) that are not of maximal order, have been dropped in (45a)-(45e).

Term in (40a)-(40e)	Contribution to (45a)-(45e)
$\ \mathbf{D}\ $	$-\hat{D}_{11}$
I	$-\frac{I^*}{\ \mathbf{D}^*\ }\hat{D}_{11} - \frac{I^*}{2p^*}\hat{p}$
$\partial_j[\tau \cos(2\psi)]$	$(\partial_p\tau)^* \partial_j\hat{p} + (\partial_\phi\tau)^* \partial_j\hat{\phi}$ $+(\partial_I\tau)^* \left\{ -\frac{I^*}{\ \mathbf{D}^*\ }\partial_j\hat{D}_{11} - \frac{I^*}{2p^*}\partial_j\hat{p} \right\}$
$\partial_j[\tau \sin(2\psi)]$	$2\tau^* \partial_j\hat{\psi}$
$f\ \mathbf{D}\ $	$-f^*\hat{D}_{11} + \ \mathbf{D}^*\ (\partial_p f)^*\hat{p} + \ \mathbf{D}^*\ (\partial_\phi f)^*\hat{\phi}$ $+\ \mathbf{D}^*\ (\partial_I f)^* \left\{ -\frac{I^*}{\ \mathbf{D}^*\ }\hat{D}_{11} - \frac{I^*}{2p^*}\hat{p} \right\}$

Table 1: *List of maximal-order linearisations of terms in (40a)-(40e), to assist in deriving (45a)-(45e). In this table only, the abbreviation $\hat{D}_{11} = (\partial_1\hat{u}_1 - \partial_2\hat{u}_2)/2$ is used.*

Putting all the pieces together, we obtain the linearisation⁷ of the system (40a)-(40e)

$$\rho_*\phi^*d_t^*\hat{u}_1 + A(-\partial_{11}\hat{u}_1 + \partial_{12}\hat{u}_2) + (\partial_\phi\tau)^*\partial_1\hat{\phi} + (1+B)\partial_1\hat{p} + 2\tau^*\partial_2\hat{\psi} = 0, \quad (45a)$$

$$\rho_*\phi^*d_t^*\hat{u}_2 + A(\partial_{12}\hat{u}_1 - \partial_{22}\hat{u}_2) - (\partial_\phi\tau)^*\partial_2\hat{\phi} + (1-B)\partial_2\hat{p} + 2\tau^*\partial_1\hat{\psi} = 0, \quad (45b)$$

$$d_t^*\hat{\phi} + \phi^*(\partial_1\hat{u}_1 + \partial_2\hat{u}_2) = 0, \quad (45c)$$

$$(1+C)\partial_1\hat{u}_1 + (1-C)\partial_2\hat{u}_2 - 2\|\mathbf{D}^*\|(\partial_\phi f)^*\hat{\phi} + \Gamma\hat{p} = 0, \quad (45d)$$

$$\partial_2\hat{u}_1 + \partial_1\hat{u}_2 + 4\|\mathbf{D}^*\|\hat{\psi} = 0, \quad (45e)$$

where

$$d_t^* = \partial_t + u_1^*\partial_1 + u_2^*\partial_2, \quad A = \frac{I^*}{2\|\mathbf{D}^*\|}(\partial_I\tau)^*, \quad B = (\partial_p\tau)^* - \frac{I^*}{2p^*}(\partial_I\tau)^*, \quad (46)$$

$$C = f^* + I^*(\partial_I f)^*, \quad \text{and} \quad \Gamma = -2\|\mathbf{D}^*\| \left((\partial_p f)^* - \frac{I^*}{2p^*}(\partial_I f)^* \right). \quad (47)$$

Observe that by hypothesis (18), $B = C$, a fact that we use in (50) and below.

⁷These equations are maximal order except that in (45a) and (45b) the term $d_t^*\hat{u}_j$ retains first-order spatial derivatives even though these equations also contain second-order derivatives of \hat{u}_j .

4 Proofs, Part II: Calculation of growth rates

4.1 The eigenvalue problem

We now look for exponential solutions of (45a)-(45e),

$$\hat{U}(\mathbf{x}, t) = e^{i\langle \boldsymbol{\xi}, \mathbf{x} \rangle + \lambda t} \tilde{U}, \quad (48)$$

where $\tilde{U} = (\tilde{u}_1, \tilde{u}_2, \tilde{\phi}, \tilde{p}, \tilde{\psi})$ is a 5-vector of scalars, $\boldsymbol{\xi} = (\xi_1, \xi_2)$ is a vector wavenumber, $\langle \cdot, \cdot \rangle$ indicates the inner product, and λ is the growth rate. The function (48) is a solution of (45a)-(45e) iff λ, \tilde{U} satisfies the generalised eigenvalue problem

$$\mathbf{S}\tilde{U} = -(\lambda + i\langle \mathbf{u}^*, \boldsymbol{\xi} \rangle)\mathbf{E}\tilde{U}, \quad (49)$$

where $\mathbf{u}^* = (u_1^*, u_2^*)$,

$$\mathbf{S} = \begin{bmatrix} A\xi_1^2 & -A\xi_1\xi_2 & i(\partial_\phi\tau)^*\xi_1 & (1+B)i\xi_1 & 2i\tau^*\xi_2 \\ -A\xi_1\xi_2 & A\xi_2^2 & -i(\partial_\phi\tau)^*\xi_2 & (1-B)i\xi_2 & 2i\tau^*\xi_1 \\ i\phi^*\xi_1 & i\phi^*\xi_2 & 0 & 0 & 0 \\ (1+B)i\xi_1 & (1-B)i\xi_2 & -2\|\mathbf{D}^*\|(\partial_\phi f)^* & \Gamma & 0 \\ i\xi_2 & i\xi_1 & 0 & 0 & 4\|\mathbf{D}^*\| \end{bmatrix}, \quad (50)$$

and

$$\mathbf{E} = \begin{bmatrix} \rho_*\phi^* & & & & \\ & \rho_*\phi^* & & & \\ & & 1 & & \\ & & & 0 & \\ & & & & 0 \end{bmatrix}. \quad (51)$$

On the right side of (49), the modified eigenvalue parameter is $\lambda + i\langle \mathbf{u}^*, \boldsymbol{\xi} \rangle$ because

$$d_t^* e^{i\langle \boldsymbol{\xi}, \mathbf{x} \rangle + \lambda t} = (\lambda + i\langle \mathbf{u}^*, \boldsymbol{\xi} \rangle) e^{i\langle \boldsymbol{\xi}, \mathbf{x} \rangle + \lambda t}.$$

Equation (49) is a *generalised* eigenvalue problem because \mathbf{E} , the matrix of coefficients of time-derivative terms, is not invertible. To extract an ordinary eigenvalue problem, we decompose \mathbf{S} into blocks

$$\mathbf{S} = \begin{bmatrix} \mathbf{S}_{11} & \mathbf{S}_{12} \\ \mathbf{S}_{21} & \mathbf{S}_{22} \end{bmatrix}, \quad (52)$$

where

$$\mathbf{S}_{11} = \begin{bmatrix} A\xi_1^2 & -A\xi_1\xi_2 & i(\partial_\phi\tau)^*\xi_1 \\ -A\xi_1\xi_2 & A\xi_2^2 & -i(\partial_\phi\tau)^*\xi_2 \\ i\phi^*\xi_1 & i\phi^*\xi_2 & 0 \end{bmatrix} \quad (53)$$

and \mathbf{S}_{12} , \mathbf{S}_{21} , and \mathbf{S}_{22} fill out the rest of the matrix. Defining $\tilde{\mathbf{U}}_1 = (\tilde{u}_1, \tilde{u}_2, \tilde{\phi})$ and $\tilde{\mathbf{U}}_2 = (\tilde{p}, \tilde{\psi})$, we rewrite (49) as

$$\begin{bmatrix} \mathbf{S}_{11} & \mathbf{S}_{12} \\ \mathbf{S}_{21} & \mathbf{S}_{22} \end{bmatrix} \begin{bmatrix} \tilde{\mathbf{U}}_1 \\ \tilde{\mathbf{U}}_2 \end{bmatrix} = -(\lambda + i\langle \mathbf{u}^*, \boldsymbol{\xi} \rangle) \mathbf{E} \begin{bmatrix} \tilde{\mathbf{U}}_1 \\ \tilde{\mathbf{U}}_2 \end{bmatrix}. \quad (54)$$

The zero entries in the last two rows of \mathbf{E} mean that $\mathbf{S}_{21}\tilde{\mathbf{U}}_1 + \mathbf{S}_{22}\tilde{\mathbf{U}}_2 = 0$ so we can solve for

$$\tilde{\mathbf{U}}_2 = -\mathbf{S}_{22}^{-1}\mathbf{S}_{21}\tilde{\mathbf{U}}_1. \quad (55)$$

Substitution of $\tilde{\mathbf{U}}_2$ into (54) then reduces this problem⁸ to the ordinary 3×3 eigenvalue problem,

$$\mathbf{E}_{11}^{-1} [\mathbf{S}_{11} - \mathbf{S}_{12}\mathbf{S}_{22}^{-1}\mathbf{S}_{21}] \tilde{\mathbf{U}}_1 = -(\lambda + i\langle \mathbf{u}^*, \boldsymbol{\xi} \rangle) \tilde{\mathbf{U}}_1 \quad (56)$$

where \mathbf{E}_{11} is the 3×3 block in the upper left of \mathbf{E} .

We decompose the 3×3 matrix in (56) into smaller blocks,

$$\begin{bmatrix} (\mathbf{M} + \mathbf{N})/\rho_*\phi^* & i\mathbf{V}/\rho_*\phi^* \\ i\phi^*\boldsymbol{\xi}^T & 0 \end{bmatrix} \tilde{\mathbf{U}}_1 = -(\lambda + i\langle \mathbf{u}^*, \boldsymbol{\xi} \rangle) \tilde{\mathbf{U}}_1 \quad (57)$$

where we calculate

$$\mathbf{M} = A \begin{bmatrix} \xi_1^2 & -\xi_1\xi_2 \\ -\xi_1\xi_2 & \xi_2^2 \end{bmatrix} \quad (58)$$

as the contribution of \mathbf{S}_{11} ,

$$\mathbf{N} = \begin{bmatrix} \frac{(1+B)^2}{\Gamma}\xi_1^2 + \frac{\tau^*}{2\|\mathbf{D}^*\|}\xi_2^2 & \frac{(1-B^2)}{\Gamma}\xi_1\xi_2 + \frac{\tau^*}{2\|\mathbf{D}^*\|}\xi_1\xi_2 \\ \frac{(1-B^2)}{\Gamma}\xi_1\xi_2 + \frac{\tau^*}{2\|\mathbf{D}^*\|}\xi_1\xi_2 & \frac{(1-B^2)}{\Gamma}\xi_2^2 + \frac{\tau^*}{2\|\mathbf{D}^*\|}\xi_1^2 \end{bmatrix}, \quad (59)$$

as the contribution of $-\mathbf{S}_{12}\mathbf{S}_{22}^{-1}\mathbf{S}_{21}$, which is symmetric, and

$$\mathbf{V} = \begin{bmatrix} \left((\partial_\phi\tau)^* + \frac{2(1+B)\|\mathbf{D}^*\|(\partial_\phi f)^*}{\Gamma} \right) \xi_1 \\ \left(-(\partial_\phi\tau)^* + \frac{2(1-B)\|\mathbf{D}^*\|(\partial_\phi f)^*}{\Gamma} \right) \xi_2 \end{bmatrix}. \quad (60)$$

4.2 Estimation of the eigenvalues

We claim that the growth-rate eigenvalues (57) satisfy

$$\max_{j=1,2,3} \sup_{\boldsymbol{\xi} \in \mathbb{R}^2} \Re\lambda_j(\boldsymbol{\xi}) < \infty.$$

By compactness, it suffices to prove that

$$\max_{j=1,2,3} \limsup_{|\boldsymbol{\xi}| \rightarrow \infty} \Re\lambda_j(\boldsymbol{\xi}) < \infty. \quad (61)$$

⁸In other words, we are performing on the symbol level the reduction that we performed on the operator level in Section 2.4.

Since only the real parts of eigenvalues matter, we may drop the term $i\langle \mathbf{u}^*, \boldsymbol{\xi} \rangle$ in (57) and verify (61) for the eigenvalue problem⁹

$$\mathbf{P}\tilde{\mathbf{U}} = -\lambda\tilde{\mathbf{U}} \quad (62)$$

where we write

$$\mathbf{P} = \begin{bmatrix} (\mathbf{M} + \mathbf{N})/\rho_*\phi^* & i\mathbf{V}/\rho_*\phi^* \\ i\phi^*\boldsymbol{\xi}^T & 0 \end{bmatrix} \quad (63)$$

for the matrix in (57) and we shorten the notation by dropping the subscript 1 on $\tilde{\mathbf{U}}$. For large $\boldsymbol{\xi}$ it is instructive to use perturbation theory to compare the eigenvalues (62) with the eigenvalues $\mathbf{P}_0\tilde{\mathbf{U}} = -\Lambda\tilde{\mathbf{U}}$ where

$$\mathbf{P}_0 = (\rho_*\phi^*)^{-1} \begin{bmatrix} \mathbf{M} + \mathbf{N} & 0 \\ 0 & 0 \end{bmatrix}. \quad (64)$$

Lemma. *Provided $\boldsymbol{\xi} \neq 0$, the 2×2 matrix $\mathbf{M} + \mathbf{N}$ is positive definite.*

Proof. Since \mathbf{M} and \mathbf{N} are symmetric, it suffices to show that the trace and determinant of $\mathbf{M} + \mathbf{N}$ are positive. According to (19), $A > 0$ and $\Gamma > 0$, from which it follows immediately that $\text{tr}(\mathbf{M} + \mathbf{N}) > 0$.

Regarding the determinant, for any 2×2 matrices

$$\det(\mathbf{M} + \mathbf{N}) = \det \mathbf{M} + \det \mathbf{N} + \chi(\mathbf{M}, \mathbf{N}), \quad (65)$$

where

$$\chi(\mathbf{M}, \mathbf{N}) = M_{22}N_{11} + M_{11}N_{22} - M_{12}N_{21} - M_{21}N_{12} \quad (66)$$

accounts for the cross terms. For the specific matrices (58) and (59), $\det \mathbf{M} = 0$,

$$\det \mathbf{N} = \frac{2\tau^*}{4\Gamma\|\mathbf{D}^*\|} [(1+B)^2\xi_1^4 - 2(1-B)\xi_1^2\xi_2^2 + (1-B)^2\xi_2^4] \quad (67a)$$

$$= \frac{2\tau^*}{4\Gamma\|\mathbf{D}^*\|} [(1+B)\xi_1^2 - (1-B)\xi_2^2]^2 \geq 0, \quad (67b)$$

and

$$\chi(\mathbf{M}, \mathbf{N}) = \frac{\tau^*}{2\|\mathbf{D}^*\|}\xi_1^4 + \left(\frac{4}{\Gamma} + \frac{\tau^*}{\|\mathbf{D}^*\|}\right)\xi_1^2\xi_2^2 + \frac{\tau^*}{2\|\mathbf{D}^*\|}\xi_2^4 > 0. \quad (68)$$

This proves the lemma. ■

Remark. It is noteworthy that $\det \mathbf{N} > 0$ except for the two directions

$$\frac{\xi_1}{\xi_2} = \pm\sqrt{\frac{1-B}{1+B}}. \quad (69)$$

Effectively, this calculation rederives the result of Pitman & Schaeffer [11] that the equations of CSSM, even without I -dependence, are well posed for all directions except possibly those defined by (69).

⁹Don't forget the minus sign in this equation—the growth rates are *negative* eigenvalues of \mathbf{P} .

It follows from the lemma that $\mathbf{P}_0 \tilde{\mathbf{U}} = -\Lambda \tilde{\mathbf{U}}$ has two eigenvalues, say Λ_1, Λ_2 , where $\Lambda_1, \Lambda_2 < 0$ and is homogenous of degree 2 in $\boldsymbol{\xi}$. Since \mathbf{P} is an $\mathcal{O}(|\boldsymbol{\xi}|)$ -perturbation of \mathbf{P}_0 , two of the growth-rate eigenvalues of (62) satisfy

$$\lambda_j = \Lambda_j + \mathcal{O}(|\boldsymbol{\xi}|), \quad j = 1, 2,$$

both of which are negative in the limit $|\boldsymbol{\xi}| \rightarrow \infty$; i.e., they are bounded above by zero in this limit. The third growth rate is given by

$$\lambda_3 = -\frac{\det \mathbf{P}}{\lambda_1 \lambda_2} = -\frac{\det \mathbf{P}}{\Lambda_1 \Lambda_2} + \mathcal{O}(|\boldsymbol{\xi}|^{-1}).$$

The first term on the extreme right is the ratio of two quartics, the denominator being nonzero, so it is bounded, and the perturbation decays at infinity. This verifies (61) for all three eigenvalues derived from (45a)-(45e).

It remains to consider the effect of the lower-order terms that were neglected in (45a)-(45e). Inclusion of these terms would lead, after a calculation as above, to an eigenvalue problem (62) for a perturbed matrix

$$\begin{bmatrix} \frac{\mathbf{M} + \mathbf{N}}{\rho_* \phi^*} + \mathcal{O}(\boldsymbol{\xi}) & \frac{i\mathbf{V}}{\rho_* \phi^*} + \mathcal{O}(1) \\ i\phi^* \boldsymbol{\xi}^T + \mathcal{O}(1) & \mathcal{O}(1) \end{bmatrix}.$$

As above, two of the eigenvalues of this matrix are negative and $\mathcal{O}(|\boldsymbol{\xi}|^2)$, and invoking the determinant shows that the third is bounded. This verifies (61) for eigenvalues of the full linearization of (40a)-(40e) and hence shows that the system is linearly well posed.

5 Conclusions and discussion

In this paper we have proposed and analysed a synthesis of critical state soil mechanics and the $\mu(I)$ -rheology. We have found that inclusion of compressibility removes the ill-posedness at low and high inertial numbers in the incompressible $\mu(I)$ equations.

Simultaneously, the result shows that the introduction of rate-dependence into CSSM, through variation of the inertial number, gives linearly well-posed equations, provided that the yield locus and flow rule satisfy (18) and (19).

Appendix 1: Ideas from Critical State Soil Mechanics

A1.1 Constitutive equations

Critical State Soil Mechanics (CSSM) is an ingeniously constructed version of plasticity that includes compressibility but reduces to a singular perturbation of Coulomb material, which is incompressible, in an appropriate limit. In two-dimensional CSSM, flow is described by the usual six variables, ϕ , \mathbf{u} ,

and $\boldsymbol{\sigma}$. Since flow is compressible, the solids fraction ϕ remains as a genuine variable. The governing equations consist of the conservation laws (1), (2) plus three constitutive laws. One of the constitutive equations is the alignment condition (8), with no changes required. The second constitutive equation, like (5), specifies the norm of the deviatoric stress,

$$\textbf{Yield condition:} \quad \|\boldsymbol{\tau}\| = Y(p, \phi), \quad (70)$$

but as indicated the function Y depends on the solids fraction ϕ as well as on the mean stress p . The final constitutive relation, the flow rule, relates expansion and contraction of material to the slope of the yield surface,

$$\textbf{Flow rule:} \quad \text{div } \mathbf{u} = 2 \frac{\partial Y}{\partial p}(p, \phi) \|\mathbf{D}\|. \quad (71)$$

We refer to Jackson [1] for a derivation of (71) from the normality condition of plasticity.

By way of example, a simple, physically acceptable, yield locus is given by

$$Y(p, \phi) = 2\mu p - p^2/C(\phi), \quad (72)$$

where μ is a coefficient of friction, as in (5), and $C(\phi)$ is an increasing function of the solids fraction of the form (29). For such a yield condition, it follows from the proof of Lemma 3, restricted to the case where $\mu(I)$ is independent of I , that equations (1), (2), (70), (71), (8) reduce to the Coulomb model in the limit $\varepsilon \rightarrow 0$.

A1.2 Consequences of the flow rule

The behaviour discussed in this subsection occurs under fairly general hypotheses—see Jackson [1]. However, to explain the theory with a minimum of technicalities, we confine the discussion to the specific yield condition (72).

The phrase *critical state*, from which CSSM derives its name, refers to a state p, ϕ such that

$$\frac{\partial Y}{\partial p}(p, \phi) = 0. \quad (73)$$

For the example yield condition (72), condition (73) means that

$$2(\mu - p/C(\phi)) = 0. \quad (74)$$

Rewriting the yield condition as $Y(p, \tau) = [2\mu - p/C(\phi)]p$ and invoking (74), we deduce that at a critical state

$$\|\boldsymbol{\tau}\| = \mu p. \quad (75)$$

The set where (75) is satisfied is called the critical state line. Thus, *along the critical state line, the stress satisfies the Coulomb yield condition.*

According to the flow rule (71), at a critical state, deformation is not accompanied by any change in ϕ . Let us examine behaviour away from the critical state line. Suppose that, for example, initially

the (uniform) state of material is at yield at the point A in Figure 2(b). At this point, $\partial Y/\partial p < 0$, so according to flow rule $\text{div } \mathbf{u} < 0$; i.e., material compactifies and becomes stronger, so τ must increase for deformation to continue. Indeed, the stress will continue to increase until a critical state on a larger yield surface is reached, as suggested in the figure by the ϕ_3 -yield surface. Moreover, if ε in (29) is small, a very slight increase in ϕ is sufficient to accommodate this evolution. I.e., we expect stress to be quickly driven from the point A to a critical state on a larger yield surface where the Coulomb yield condition (75) is satisfied.

Conversely, at point B in the figure, $\partial Y/\partial p > 0$, so under deformation $\text{div } \mathbf{u} > 0$; i.e., material expands and becomes weaker. It is natural to imagine that the stress is driven to a critical state on a smaller yield surface, as suggested by the arrow in the figure. This would indeed be the case *if material deformed uniformly*, but this assumption is unrealistic for stresses above the critical state line, $\tau > \mu p$. For such stresses, because material expands under deformation and therefore weakens, instability often causes localised deformation—if deformation near one point happens to be slightly larger than elsewhere, the associated expansion lowers the yield condition more near this point, and subsequent deformation tends to concentrate near this point.

Appendix 2: A primer on ill posed PDEs

The following appendix gives a self-contained, elementary summary of key issues regarding ill-posed PDEs. A much more detailed treatment can be found in Joseph & Saut [6].

A2.1 Testing for ill-posedness

The initial value problem for a PDE is called *well posed* in the sense of Hadamard if for general initial data a solution (1) exists, (2) is unique and (3) varies continuously under perturbations of the initial conditions¹⁰ (cf. also Pinchover & Rubinstein [27]). If one or more of these criteria is not satisfied then the problem is called *ill posed*. A classic example of an ill-posed problem is the backward heat equation

$$\partial_t u = -\partial_{xx} u. \tag{76}$$

In Section A2.2 below we show Condition (1) fails; here we show Condition (3) also fails. Taking the Fourier transform reveals that the equation admits solutions

$$u_\xi(x, t) = \sin(\xi x) e^{\xi^2 t}, \tag{77}$$

¹⁰More precisely regarding Condition (1): we choose a positive integer k and require that the IVP has a solution for any initial conditions in $\mathcal{BC}^k(\mathbb{R}^n)$, i.e., for k -times continuously differentiable functions such that all derivatives of order k or less are bounded. Likewise regarding Condition (3): we require that for the same integer k and for any positive time T , the solution operator is continuous as a map from $\mathcal{BC}^k(\mathbb{R}^n)$ into continuous functions on $[0, T] \times \mathbb{R}^n$. We refer to Joseph & Saut [6] for elaboration of these issues.

for any $\xi \in \mathbb{R}$. Consider the scaled solutions $|\xi|^{-p}u_\xi(x, t)$, where $p > 0$, as perturbations of the trivial solution $u(x, t) \equiv 0$. The initial conditions of the scaled solution—i.e., $|\xi|^{-p} \sin(\xi x)$ —tend to zero in the sup norm as $\xi \rightarrow \infty$; indeed, if $p > k$ these initial conditions tend to zero in the \mathcal{C}^k norm. On the other hand, for any $t > 0$ the norm

$$\sup_{x \in \mathbb{R}} |\xi|^{-p} u_\xi(x, t) \quad (78)$$

tends to infinity in this limit. Thus, an arbitrarily small perturbation of initial conditions for (76) can lead to an arbitrarily large solution in an arbitrarily short time.

For more general PDEs there is a test for ill-posedness based on Fourier analysis of the *linearisation* of the equations. The process is summarised as:

1. Linearise the equations about a base-state solution;
2. Freeze the coefficients at some point (\mathbf{x}^*, t^*) ;
3. Look for solutions with exponential dependence $e^{i\langle \boldsymbol{\xi}, \mathbf{x} \rangle + \lambda(\boldsymbol{\xi})t}$.

We shall say the original PDE is linearly ill-posed (with respect to the base-state solution at the given point) if

$$\limsup_{|\boldsymbol{\xi}| \rightarrow \infty} \lambda(\boldsymbol{\xi}) = +\infty.$$

For most examples, if a PDE is linearly ill-posed, it is ill posed in the sense of Hadamard. (But see Kreiss [28] for exceptional examples.)

An equation is called *linearly well-posed* with respect to a given base solution if the growth rate is bounded from above for all points (\mathbf{x}^*, t^*) . Linear well-posedness does not imply well-posedness in the sense of Hadamard. For example, it is trivially verified that the Navier-Stokes equations are linearly well-posed, but a major effort is required to show that, even just for a finite time, they are well posed in the sense of Hadamard, and it is not known whether they are well posed for all time.

We illustrate the above test on the following made-up nonlinear system that has some similarity to the PDEs analysed in this paper,

$$\begin{aligned} \partial_t u &= \partial_x v, \\ \partial_t v &= \varepsilon u \partial_{xx} v + \partial_x u - v - \sin(x). \end{aligned} \quad (79)$$

The linearised equations with frozen coefficients are

$$\begin{aligned} \partial_t \hat{u} &= \partial_x \hat{v}, \\ \partial_t \hat{v} &= \varepsilon [u^* \partial_{xx} \hat{v} + (\partial_{xx} v)^* \hat{u}] + \partial_x \hat{u} - \hat{v}, \end{aligned} \quad (80)$$

where u^*, v^* is the base-state solution evaluated at the point (x^*, t^*) and \hat{u}, \hat{v} are the perturbations. These constant-coefficient linear PDEs have exponential solutions

$$\hat{\mathbf{U}} = \begin{bmatrix} \hat{u} \\ \hat{v} \end{bmatrix} = e^{i\xi x + \lambda t} \tilde{\mathbf{U}}, \quad (81)$$

where $\tilde{U} \in \mathbb{R}^2$ satisfies the eigenvalue problem

$$\begin{bmatrix} 0 & i\xi \\ i\xi + \varepsilon \partial_{xx} v^* & -\varepsilon u^* \xi^2 - 1 \end{bmatrix} \tilde{U} = \lambda \tilde{U}. \quad (82)$$

The eigenvalues of (82) could be easily calculated exactly but, provided that $u^* \neq 0$, they can be estimated more easily from their asymptotic behaviour as $|\xi| \rightarrow \infty$:

$$\lambda_1 = -\varepsilon u^* \xi^2 + \mathcal{O}(\xi) \quad \text{and} \quad \lambda_2 = \frac{\det S(\xi)}{\lambda_1} = -\frac{1}{\varepsilon u^*} + \mathcal{O}(\xi^{-1}). \quad (83)$$

where $S(\xi)$ is the 2×2 matrix in (82). If $u^* > 0$, then the eigenvalues satisfy

$$\max_{j=1,2} \limsup_{|\xi| \rightarrow \infty} \Re \lambda_j(\xi) < \infty, \quad (84)$$

so (79) is linearly well posed. On the other hand if $u^* < 0$, then λ_1 is unbounded, so (79) is ill posed.

Note that in analysing linear ill-posedness of (79) we consider the *full* linearization of the equations, i.e., (80). One might be tempted to discard terms with lower-order derivatives in the expectation that the growth of exponential solutions as $|\xi| \rightarrow \infty$ ought to be dominated by the highest-order derivatives in the equation. However, the counter-example

$$\partial_t u = \partial_{xxx} u - \partial_{xx} u$$

shows this expectation is not valid in general.

Nevertheless, for this example we may in fact analyse exponential solutions of (80) by first considering the *maximal order* linearised equations

$$\begin{aligned} \partial_t \hat{u} &= \partial_x \hat{v}, \\ \partial_t \hat{v} &= \varepsilon u^* \partial_{xx} \hat{v} + \partial_x \hat{u}. \end{aligned} \quad (85)$$

In each equation of (85), only terms of maximal order are retained, i.e., the terms $(\partial_{xx} v)^* \hat{u}$ and \hat{v} have been dropped from the second equation because it contains the higher-order terms $\partial_x \hat{u}$ and $u^* \partial_{xx} \hat{v}$, respectively. The growth rate of exponential solutions of (85) satisfy the same estimates (83), and the neglected lower-order terms don't change the leading-order behaviour. Often calculations may be simplified by studying the maximal-order linearization as an intermediate step.

A2.2 Consequences of ill-posedness

A2.2.1 Restrictions on the existence of solutions

In order for an ill-posed initial value problem to have a solution, usually the initial conditions must satisfy an extreme smoothness requirement, stronger than is physically acceptable in most applications. It may be difficult to demonstrate this behaviour in general, but for the backwards heat equation, we illustrate the behaviour with

Proposition. *If $\varepsilon \neq 0$, the initial value problem for (76) with initial data $u(x, 0) = \varepsilon |\sin x|^p$ has no solution for any positive time interval unless the power p is an even non-negative integer.*¹¹

Proof. Suppose the 2π -periodic function $f(x)$ has Fourier series $f(x) \sim \sum c_n e^{inx}$. If equation (76) with initial condition $u(x, 0) = f(x)$ has a continuous solution for $0 \leq t < \eta$, it has the Fourier-series representation

$$u(x, t) = \sum_{n=-\infty}^{\infty} c_n e^{inx+n^2 t}.$$

Moreover for $0 \leq t < \eta$,

$$\sum_{n=-\infty}^{\infty} e^{2n^2 t} |c_n|^2 = \frac{1}{2\pi} \int_{-\pi}^{\pi} |u(x, t)|^2 dx < \infty. \quad (86)$$

Now if the Fourier coefficients of a function $f(x)$ satisfy $\sum n^{2k} |c_n|^2 < \infty$, then the derivatives $(d/dx)^j f(x)$ are square integrable for $j = 0, 1, \dots, k$. But, provided p is not an even non-negative integer, the proposed initial data $|\sin x|^p$ has singular behaviour near $x = 0$. Specifically, $(d/dx)^k |\sin x|^p$ is square integrable only if $k < p + 1/2$. It follows for the Fourier coefficients of $|\sin x|^p$ that if $k > p + 1/2$,

$$\sum_{n=-\infty}^{\infty} n^{2k} |c_n|^2 = \infty.$$

This inequality is incompatible with (86), so the initial value problem cannot be solved on any positive time interval. ■

A2.2.2 Grid-dependent computations

The attempt to solve an ill posed PDE numerically produces unreliable, grid dependent, results. Such behaviour has been observed in various physical problems [7, 8, 9] where the formulation was based on an ill-posed system of equations. However, in complicated problems like these, usually computational resources are stretched to the limit, meaning behaviour under grid refinement cannot be readily probed. Let us illustrate grid dependence on a much less demanding problem, the toy problem (79) above.

If $\varepsilon = 0$ and with initial conditions

$$u(x, 0) = a, \quad v(x, 0) = -\sin(x)/2, \quad (87)$$

the (linear) equations (79) have the exact solution

$$\begin{aligned} u(x, t) &= \frac{e^{-t/2}}{2} [\cos(x + \sqrt{3t}/2) + \cos(x - \sqrt{3t}/2)] + a - \cos x \\ v(x, t) &= \frac{e^{-t/2}}{2} [\cos(x + \sqrt{3t}/2 + \pi/6) - \cos(x - \sqrt{3t}/2 - \pi/6)]. \end{aligned} \quad (88)$$

The large-time limit of these solutions,

$$u(x, \infty) = a - \cos x, \quad v(x, \infty) = 0, \quad (89)$$

¹¹Of course the general solution of (76) is a linear superposition of the solutions (77). We have no need for the general solution since one counterexample is sufficient to invalidate Condition (1) above.

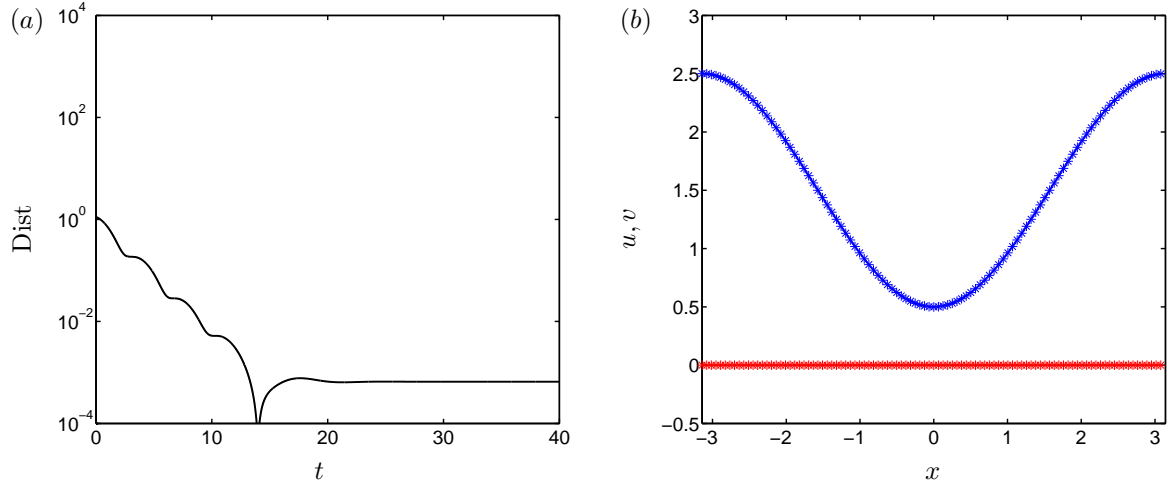


Figure 4: Numerical solutions of (79) with the distance from the asymptotic solution (90) in (a) and the fields at $t = 100$ in (b). Here $a = 1.5$, $\varepsilon = 0.01$ and the discretisation is $\Delta x = 2\pi/100$ and $\Delta t = 1 \times 10^{-3}$.

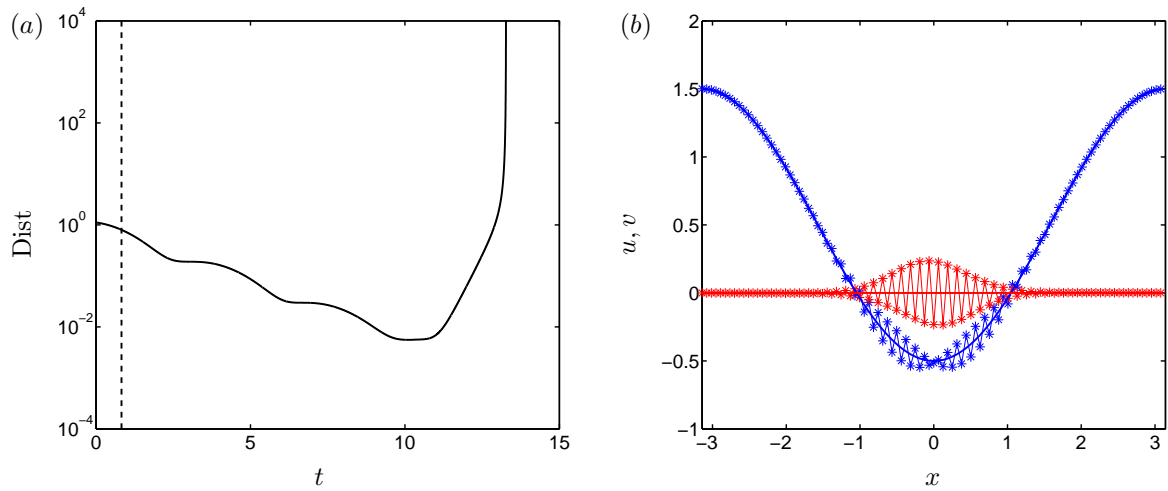


Figure 5: Numerical solutions of (79) with the distance from the asymptotic solution (90) in (a) and the fields at $t = 12.5$ in (b). Here $a = 0.5$, $\varepsilon = 0.01$ and the discretisation is $\Delta x = 2\pi/100$ and $\Delta t = 1 \times 10^{-3}$. The vertical dashed line in (a) is the first time that $u = 0$.

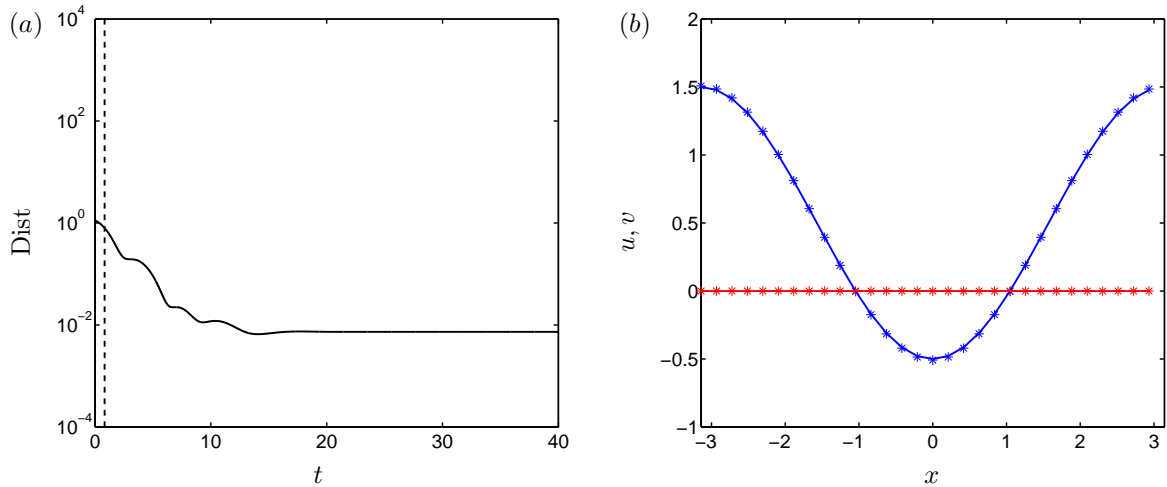


Figure 6: Numerical solutions of (79) with the distance from the asymptotic solution (90) in (a) and the fields at $t = 100$ in (b). Here $a = 0.5$, $\varepsilon = 0.01$ and the discretisation is $\Delta x = 2\pi/30$ and $\Delta t = 1 \times 10^{-3}$. The vertical dashed line is the first time that $u = 0$.

is also a steady-state solution of the nonlinear system (with $\varepsilon > 0$). If $a > 1$, then $u(x, \infty) > 0$, and the calculations above suggest that the equations will be linearly well-posed. However if $a < 1$, then $u(x, \infty)$ dips below zero over an interval, which suggests that the equations will be ill-posed.

Figure 4, where $a = 1.5$, and Figure 5, where $a = 0.5$, confirm these expectations. They show numerical solutions using a central-space forward-time explicit scheme on the periodic domain $x \in [-\pi, \pi]$ with a spatial resolution of $\Delta x = 2\pi/100$. Each figure has two panels, one showing the temporal evolution of the distance from the asymptotic solution,

$$\text{Dist} = \max \left\{ \sqrt{|u - u(x, \infty)|^2 + |v - v(x, \infty)|^2} \right\}, \quad (90)$$

and the other plotting the two variables u, v at a specific (late) time during the computation. In Figure 4, the well posed case, the numerical solution converges to the predicted steady state solution (89) within numerical accuracy. By contrast, in Figure 5, after an initial decay, ill-posedness asserts itself and causes the solution to blow up.

Regarding grid dependence, Figure 6 shows another computation in the ill posed case with a coarser grid, $\Delta x = 2\pi/30$. The solution appears to converge to the steady state solution, just like in the well posed case. In other words, the computations on the coarse grid hide the ill posed character of the underlying PDEs. This highlights that in order to extract meaningful information from numerical computations, a proper study of grid convergence must be first carried out.

Incidentally, if the grid is made finer than in Figures 4 and 5, in the well posed case $a > 1$ the numerical solution converges to the steady-state solution with a smaller numerical error, while in the ill-posed case it blows up *sooner*, as expected.

Acknowledgements

This research was supported by NERC grants NE/E003206/1 and NE/K003011/1 as well as EPSRC grants EP/I019189/1, EP/K00428X/1 and EP/M022447/1. J.M.N.T.G. is a Royal Society Wolfson Research Merit Award holder (WM150058) and an EPSRC Established Career Fellow (EP/M022447/1). Research of M.S. was supported by National Science Foundation grant DMS-1517291.

References

- [1] Jackson R. Some mathematical and physical aspects of continuum models for the motion of the granular materials. In Theory of dispersed multiphase flow. R. Meyer, Academic Press; 1983.
- [2] Schaeffer D. Instability in the evolution-equations describing incompressible granular flow. J Differ Equ. 1987;66(1):19–50.
- [3] Schaeffer DG, Pitman EB. Ill-posedness in three-dimensional plastic flow. Comm Pure Appl Math. 1988;41(7):879–890.
- [4] GDR MiDi. On dense granular flows. Eur Phys J E. 2004;14(4):341–365.
- [5] Jop P, Forterre Y, Pouliquen O. A constitutive relation for dense granular flows. Nature. 2006;44:727–730.
- [6] Joseph DD, Saut JC. Short-wave instabilities and ill-posed initial-value problems. Theor Comput Fluid Dyn. 1990;1:191–227.
- [7] Gray JMNT. Loss of hyperbolicity and ill-posedness of the viscous-plastic sea ice rheology in uniaxial divergent flow. J Phys Oceanog. 1999 NOV;29(11):2920–2929.
- [8] Woodhouse MJ, Thornton AR, Johnson CG, Kokelaar BP, Gray JMNT. Segregation-induced fingering instabilities in granular free-surface flows. J Fluid Mech. 2012;709:543–580.
- [9] Barker T, Schaeffer DG, Bohorquez P, Gray JMNT. Well-posed and ill-posed behaviour of the $\mu(I)$ -rheology for granular flow. J Fluid Mech. 2015;779:794–818.
- [10] Mandel J. Conditions de stabilité et postulate de Drucker. Rheology and Soil Mechanics, eds Kravtchenko, G and Sirieys, P. 1964;p. 58–68.
- [11] Pitman EB, Schaeffer DG. Stability of time dependent compressible granular flow in two dimensions. Communications on Pure and Applied Mathematics. 1987;40(4):421–447.

- [12] de Coulomb CA. Essai sur une application des rgles de maximis & minimis quelques problmes de statique, relatifs l'architecture. Mem Math Acad R Sci, Paris. 1773;7:343–382.
- [13] da Cruz F, Emam S, Prochnow M, Roux J, Chevoir F. Rheophysics of dense granular materials: Discrete simulation of plane shear flows. Phys Rev E. 2005;72:021309.
- [14] Pitman EB. The stability of granular flow in converging hoppers. SIAM Journal On Applied Mathematics. 1988;48:1033–1053.
- [15] Kamrin K. Nonlinear elasto-plastic model for dense granular flow. Int J Plasticity. 2010;26:167–188.
- [16] Jiang Y, Liu M. From elasticity to hypoplasticity: dynamics of granular solids. Physical review letters. 2007;99(10):105501.
- [17] Pouliquen O, Forterre Y. A non-local rheology for dense granular flows. Phil Trans R Soc A. 2009;367:5091–5107.
- [18] Kamrin K, Koval G. Nonlocal constitutive relation for steady granular flow. Phys Rev Lett. 2012;108(17):178301.
- [19] Kamrin K, Henann D. Nonlocal Modeling of Granular Flows Down Inclines. Soft Matter. 2015;11(1):179–185.
- [20] Bouzid M, Trulsson M, Claudin P, Clément E, Andreotti B. Nonlocal Rheology of Granular Flows across Yield Conditions. Phys Rev Lett. 2013;111(23):238301.
- [21] Jenkins JT, Savage SB. A theory for the rapid flow of identical, smooth, nearly elastic, spherical-particles. J Fluid Mech. 1983;130:187–202.
- [22] Harris D, Grekova EF. A hyperbolic well-posed model for the flow of granular materials. J Eng Math. 2005;52:107–135.
- [23] Sun J, Sundaresan S. A constitutive model with microstructure evolution for flow of rate-independent granular materials. J Fluid Mech. 2011;682:590–616.
- [24] Wu W, Bauer E, Kolymbas D. Hypoplastic constitutive model with critical state for granular materials. Mech Mater. 1996;23(1):45–69.
- [25] Perzyna P. Fundamental problems in viscoplasticity. Advances in applied mechanics. 1966;9:243–377.
- [26] Jop P, Forterre Y, Pouliquen O. Crucial role of sidewalls in granular surface flows: consequences for the rheology. J Fluid Mech. 2005;541:167.

- [27] Pinchover Y, Rubinstein J. An Introduction to partial differential equations. Cambridge University Press; 2005.
- [28] Kreiss HO. Numerical methods for solving time-dependent problems for partial differential equations. Presses Univ. Montréal; 1978.